TAO, Vol. 12, No. 4, 685-693, December 2001

NOTES AND CORRESPONDENCE

Traveltime Analysis of VSP Seismograms in a Horizontal Transversely Isotropic Medium: A Physical Modeling Result

Young-Fo Chang[1,*] and Chih-Hsiung Chang[2]

(Manuscript received 7 November 2000, in final form 30 August 2001)

ABSTRACT

In order to investigate the effects of anisotropy in a VSP survey, the multi-component VSP data for observing the qP-, qSH- and qSV-waves were collected with two different source-to-well offsets in an elastic transversely isotropic medium (TIM) with a horizontal symmetry axis (HTI). The traveltimes of the events were then computed using two different algorithms: first with elastic constants of the medium, and second with "isotropic velocities". Comparing the traveltimes of computations with the recorded data, a very clear and important consequence can be derived. For strongly anisotropic media (the anisotropy for the qP- and qS-waves are 25% and 29%, respectively, in our laboratory work), the effects of anisotropy increase with increasing source-to-well offset. As the source-to-well offset is small compared with the depth of the receiver (offset/depth ≤ 0.2 in our work), the effects of anisotropy can be ignored. However, in processing a large source-to-well offset VSP survey (offset/depth ≥ 0.35 in this study), special attention must be paid on the effects of anisotropy.

(Keyword: Anisotropy, Vertical seismic profile, Physical modeling)

1. INTRODUCTION

Much of the earth's crust appears to be more or less anisotropic (Crampin 1981; Crampin and Lovell 1991; Helbig 1993), making seismic wave propagation more complicated than in isotropic media. Increasing demand for fossil fuels and minerals has encouraged geophysicists to explore deep and small reservoirs that could be possibly missed by traditional techniques.

[1]Institute of Applied Geophysics, Institute of Seismology, National Chung Cheng University, Min-hsiung, Chia-yi, Taiwan, ROC

[2]Department of Applied Physics, National Chiayi University, Min-hsiung, Chia-yi, Taiwan, ROC

[*]*Corresponding author address*: Prof. Young-Fo Chang, Institute of Applied Geophysics, Institute of Seismology, National Chung Cheng University, Min-hsiung, Chia-yi 621, Taiwan, ROC

E-mail: seichyo@eq.ccu.edu.tw

Therefore, seismic exploration techniques are being extended from simple isotropic models to complex anisotropic models in order to construct the geological structures in more detail

Among seismic exploration techniques, the vertical seismic profile (VSP) is the most powerful one for investigation of anisotropy and the lithology around the well can be clearly studied. Shear-wave splitting in the near-surface late Tertiary shale is clear in both crosshole and VSP data (Winterstein and Paulsson 1990). Recorded as the components in the principal anisotropic axis, the shear-waves of different polarities reveal different velocities and reflection coefficients (Lynn and Thomsen 1990). The effects of singularities in sedimentary basins were observed in examining the shear-wave splitting in multi-offset VSPs at a borehole site in the Paris Basin (Bush and Crampin 1991). Shear-wave splitting was observed on 3-component seismograms from earthquakes of 5 to 18 km depths in the crystalline basement beneath the Los Angeles basin (Li et al. 1994). Wide-aperture walkaway VSP data acquired through transversely isotropic horizontal layers can be used to determine the qP-wave phase-slowness surface (Sayers 1997). Multi-component VSPs may reveal a strong vertical birefringence near the surface (MacBeth et al. 1997).

However, due to geological complexity and the limitation of sources and receivers, the anisotropic characteristics of the earth can not be easily identified or quantified from field data, but they can be observed in physical modeling. Ebrom et al. (1990) used a wave propagation experiment in a fractured medium to show that the moveout curves for a survey line oriented parallel to the fractures are hyperbolic, but those for a survey line oriented perpendicular to the fractures are non-hyperbolic. Cheadle et al. (1991) used industrial phenolite to study the propagations of seismic waves in an orthorhombic anisotropic medium. Brown et al. (1991) showed that the effect of the shear-wave window and the variation of the hyperbolic NMO parameter with offset are clearly observed in ultrasonic waves propagation through an orthorhombic medium. Chang et al. (1994) clearly demonstrated the phenomena of shear-wave splitting in a transversely isotropic medium (TIM). Chang and Gardner (1997) investigated the effects of subsurface fractures in a three-layer medium and observed that the horizontal moveout velocity decreases from the strike direction toward the transverse direction of the fractures.

In this paper, we study the effects of anisotropy on VSP data using physical models. The observed anisotropic traveltimes in a strongly TIM (phenolite) with a horizontal symmetry axis (HTI) are compared with its theoretical anisotropic traveltimes and the isotropic traveltimes for two different source-to-well geometries.

2. EXPERIMENTS

Vertical fractures caused by the horizontal pressure or tension force of the earth are commonly seen in the geological strata, giving the strata HTI for the seismic waves. In this study, a strongly anisotropic phenolite, composed of layers of paper bonded with phenolic resin, was used to simulate a HTI stratum. This phenolite is transversely isotropic because the paper is made up of no preferred direction. The configuration of the model, apparatus and arrangement of the measurements are shown in Fig. 1.

The pulser/receiver (Panametrics 5058PR) emits high pulse voltage to excite the transducer,

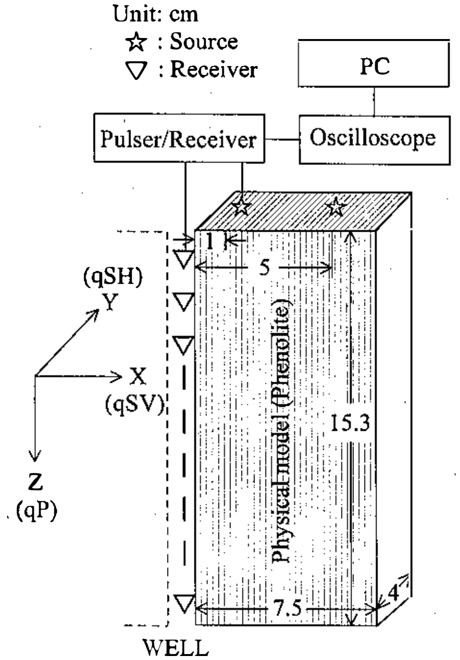

Fig. 1. Configuration of the physical modeling, arrangement of the sources and receiver, apparatus and directions used in this study.

and then receives and amplifies the weak signals. An orthogonal coordinate was adopted to describe the polarizations of the waves (Fig. 1). The Z-axis is vertical. The X- and Y-axes are horizontal and are perpendicular and parallel to the vertical fractures, respectively. A pair of small transducers of 0.25 inch diameter was used as source and receiver (Panametrics A133S for detecting in-line particle motion, and Ultran SWC18-5 for detecting off-line and perpendicular particle motion). The source-transducer emits an ultrasonic pulse into the medium and the echo is detected by the receiver-transducer. The oscilloscope (Tektronix TDS 420) receives the data and converts the analogic data into digital data. A personal computer is used to record and process the digital data.

The bulk density of phenolite is 1.4 g/cm^3. The elastic constants of the phenolite normalized by the density are A_{11}=15.8, A_{13}=5.0, A_{33}=8.7, A_{44}=2.2, and A_{66}=4.5 (10^6 m^2/s^2) (Chang and Chang 2001a). The experimental error of velocity in the experiment is within 1%. The velocity-anisotropies ((Vmax-Vmin)/Vmax) of the qP- and qS-waves for the phenolite are 25% and 29%, respectively.

3. RESULTS

The sources were located on the top surface and the receivers were located in the well. The length and time have been rescaled to simulate field seismic data, and the length and time scale factors are 10000:1. Two source-to-well offsets, 100 and 500 m, were used. The receivers were located between 100 and 1450 m depth with an interval of 50 m. Since the transducers are small relative to the propagation distance of the wave, the transducers can be considered as points. As the dominant polarizations are in the Z direction, the dominant events that are the qP-waves in this profile can be observed. When the dominant polarizations are in the Y and X directions, the dominant events that are the qSH- and qSV-waves, respectively, can be observed. The VSPs with 100 m source-to-well offset for qP-, qSH- and qSV-waves are shown in Figs. 2, 3 and 4, respectively. And the VSPs with 500 m source-to-well offset for qP-, qSH- and qSV-waves are shown in Figs. 5, 6 and 7, respectively.

The exact phase velocities of the body waves in a homogeneous TIM can be derived from the equations of motion. However, the group velocity can not be derived for a wave radiated from a point source. But it can be obtained from the phase velocity using a differential operator (Thomsen 1986). The solid lines in Figs. 2-7 are the theoretical traveltimes for the waves propagation in the phenolite with group velocities. To view the effects of the anisotropy on the propagation of elastic body waves in a HTI, the traveltimes of the elastic body waves propagation with isotropic velocities were computed for comparison. The isotropic velocities are the qP-, qSH-, and qSV-waves velocities in the Z-axis direction; they are 4000, 2100 and 1500 m/s, respectively. The dashed lines in Figs. 2-7 show the traveltimes of the waves computed with the isotropic velocities. The phenomenon of velocity cusps for qSV-waves in a HTI can be expected to show up in Fig.7 as the receivers are 400-500 m in depth by the solid line.

4. DISCUSSION AND CONCLUSIONS

The P-waves are easier to generate and detect than the S-waves in both field and laboratory. Therefore, the qP-waves can be easily and clearly observed in the experimental data (Figs. 2

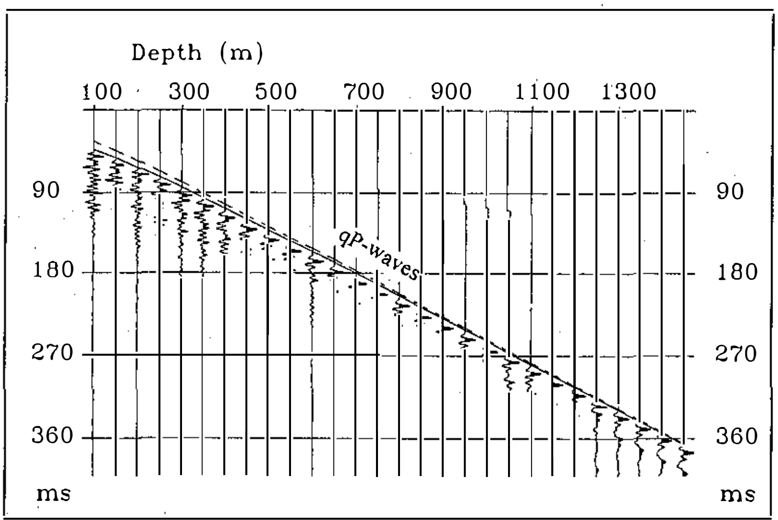

Fig. 2. The Z-Z component VSP with 100 m source-to-well offset. The dominant events in the profile are the qP-waves. The solid line is the theoretical traveltimes of the qP-waves and the dashed line is the traveltimes for the P-waves propagation using an isotropic velocity.

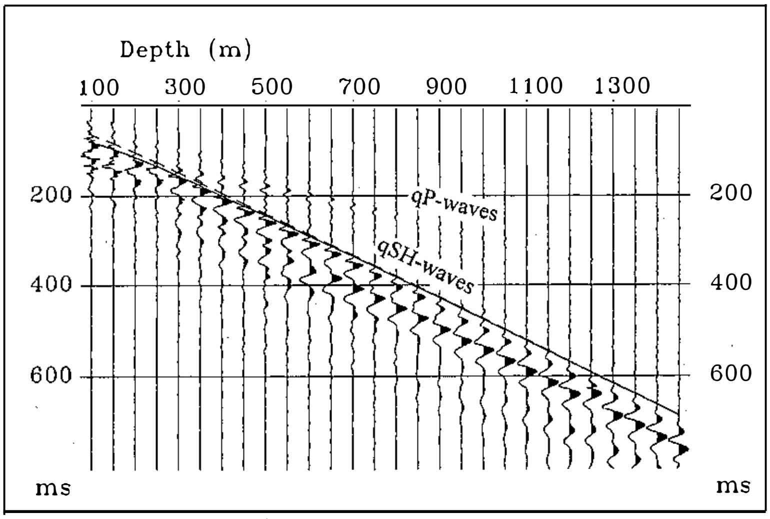

Fig. 3. The Y-Y component VSP with 100 m source-to-well offset. The dominant events in the profile are the qSH-waves. The solid line is the theoretical traveltimes of the qSH-waves and the dashed line is the traveltimes for the SH-waves propagation using an isotropic velocity.

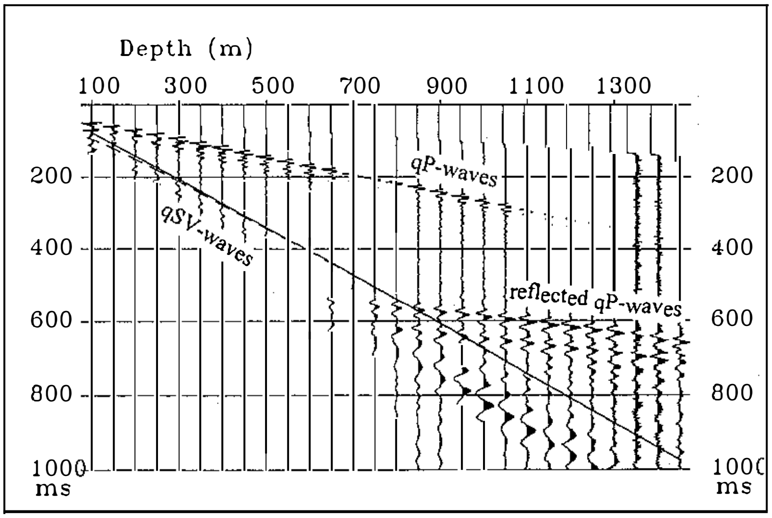

Fig. 4. The X-X component VSP with 100 m source-to-well offset. The qSV-waves are weak and can only be observed in the shallow traces. The reflected qP-waves are the qP-waves reflected from the face opposite to that the receivers located. The solid line is the theoretical traveltimes of the qSV-waves and the dashed line is the traveltimes for the SV-waves propagation using an isotropic velocity.

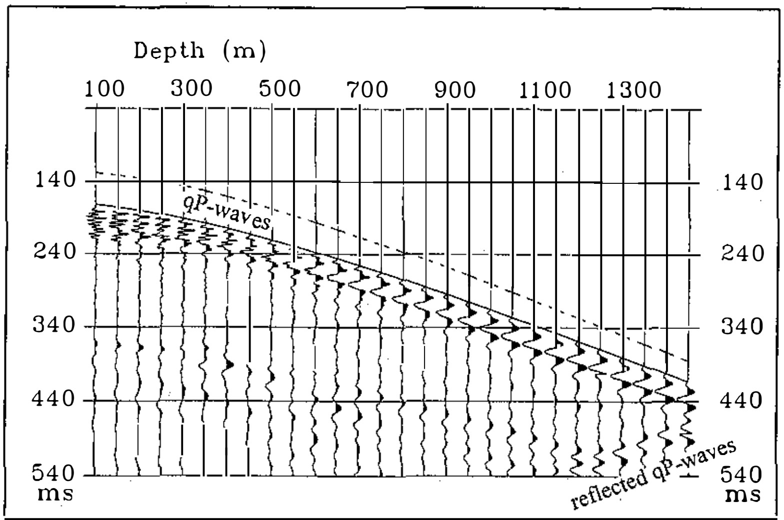

Fig. 5. The Z-Z component VSP with 500 m source-to-well offset. The dominant events in the profile are the qP-waves. The reflected qP-waves are the qP-waves reflected from the bottom of the model. The solid line is the theoretical traveltimes of the qP-waves and the dashed line is the traveltimes for the P-waves propagation using an isotropic velocity.

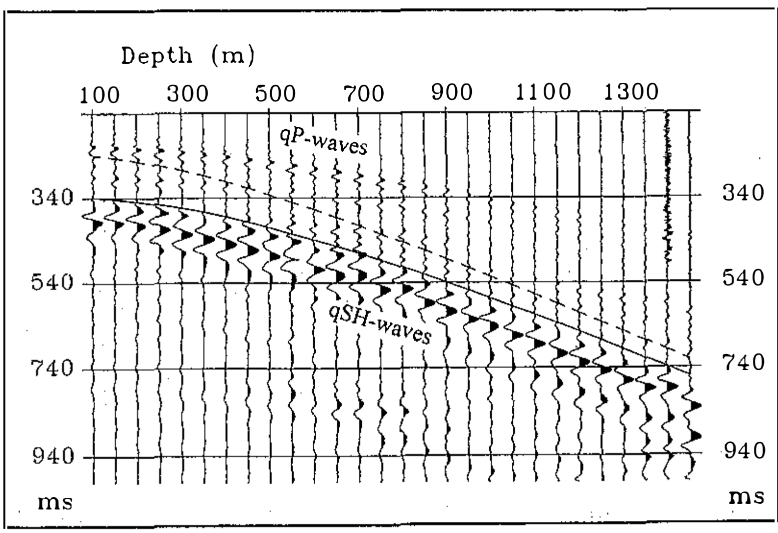

Fig. 6. The Y-Y component VSP with 500 m source-to-well offset. The dominant events in the profile are the qSH-waves. The solid line is the theoretical traveltimes of the qSH-waves and the dashed line is the traveltimes for the SH-waves propagation using an isotropic velocity.

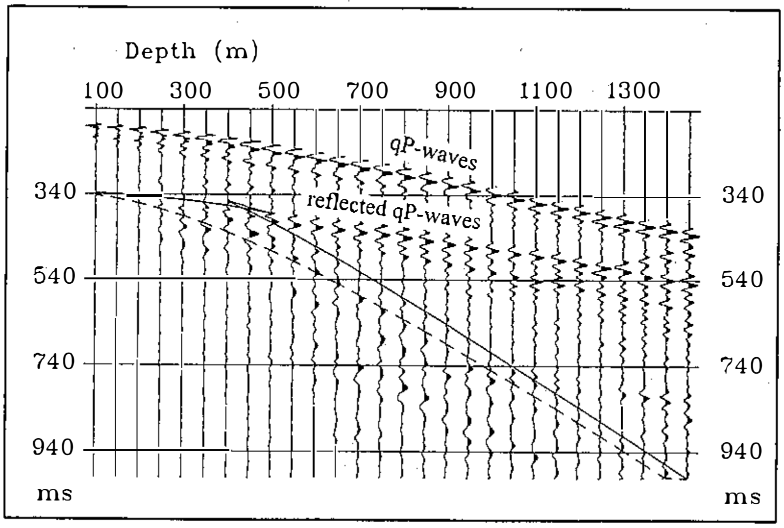

Fig. 7. The X-X component VSP with 500 m source-to-well offset. The qSV-waves are too obscure to be observed. The reflected qP-waves are the qP-waves reflected from the face opposite to that the receivers located. The solid line is the theoretical traveltimes of the qSV-waves and the dashed line is the traveltimes for the SV-waves propagation using an isotropic velocity.

and 5). The qSH-waves are irreverent to qP- and qSV-waves. Hence, qSH-waves can be seen in Figs. 3 and 6; however, they are blurrier than qP-wave VSPs, and the small amplitude and high frequency converted qP-waves arrive before the qSH-waves. Although the same transducers are used for measuring the qSH- and qSV-waves, with a 90 degree difference in polarization, the qSV-waves show an obstacle in the recorded data (Figs. 4 and 7). The qSV-waves are generally noisier than the qSH-waves in the ultrasonic transmission experiments. This is because the attenuation of medium for the qSV-wave is stronger than the qSH-wave, and the qSV-wave is somewhat like to convert to qP-wave. Although the qSV-waves are obscure and are contaminated by the direct qP-waves and converted qP-waves, they still can be recognized in the shallow traces of Fig. 4; but in Fig. 7 they are too weak to be observed. In Figs. 2-6, the good agreement between the theoretical (solid lines) and observed traveltimes confirms that the events we observed are the quasi body waves propagating with the group velocity. The isotropic arrivals advanced those of the anisotropic arrivals (in Figs. 2-3 and 5-6) is because that the isotropic velocities (P- and S-waves) used in this study are the maximum velocities of the qP- and qSH-waves. But the isotropic velocity of the SV-waves is not the maximum velocity of the qSV-wave (Figs. 4 and 7).

When the source-to-well offset is small (offset/depth ≤ 0.2 in our work), it can be seen that the curves of the predicted arrivals of the quasi body waves in our modeling HTI fit the ones that were computed using the isotropic velocities (Figs. 2-4), especially for depths greater than 500 m. The departure between these curves becomes smaller as the receiver runs deeper. As the source-to-well offset is increased (offset/depth ≥ 0.35 in this study) (Figs. 5-7) or the depth of the small offset VSPs is reduced (Figs. 2-4), deviation between the curves of arrivals that are respectively computed from the elastic constant and isotropic velocities is also increased. The conclusion thus can be drawn that the idea of isotropic velocity can be confidently applied to the processing of VSP data when the offset of the source to the well is small relative to the depth of the receiver. For a relatively large offset, the effects of anisotropy must be taken into account in the processing of VSP data. Otherwise, the VSP data can be erroneously processed and interpreted.

Acknowledgment This research was financially supported by the National Science Council under the contract no. NSC 89-2116-M-194-004.

REFERENCES

Brown, R. J., D. C. Lawton, and S. P. Cheadle, 1991: Scaled physical modelling of anisotropic wave propagation: Multioffset profiles over an orthorhombic medium. *Geophys. J. Int.*, **107**, 693-702.

Bush, I., and S. Crampin, 1991: Paris Basin VSPs: case history establishing combinations of fine-layer (or lithologic) anisotropy and crack anisotropy from modelling shear wavefields near point singularities. *Geophys. J. Int.*, **107**, 433-477.

Chang, C. H., G. H. F. Gardner, and J. A. McDonald, 1994: A physical model of shear-wave propagation in a transversely isotropic solid. *Geophysics*, **59**, 484-487.

Chang, C. H., and G. H. F. Gardner, 1997: Effects of vertically aligned subsurface fractures on seismic reflections: A physical model study. *Geophysics*, **62**, 245-252.

Chang, Y. F., and C. H. Chang, 2001a: Laboratory results for the features of body wave propagation in a transversely isotropic medium. *Geophysics*, in press.

Cheadle, S. P., R. J. Brown, and D. C. Lawton, 1991: Orthorhombic anisotropy: A physical seismic modeling study. *Geophysics*, **56**, 1603-1613.

Crampin, S., 1981: A review of wave motion in anisotropic and cracked elastic-media. *Wave motion*, **3**, 343-391.

Crampin, S., and J. H. Lovell, 1991: A decade of shear-wave splitting in the earth's crust: what does it mean? what use can we make of it? and what should we do next ? *Geophys. J. Int.*, **107**, 387-407.

Ebrom, D. A., R. H. Tatham, K. K. Sekharan, J. A. McDonald, and G. H. F. Gardner, 1990: Hyperbolic traveltime analysis of first arrivals in an azimuthally anisotropic medium: A physical modeling study. *Geophysics*, **55**, 185-191.

Helbig, K., 1993: Simultaneous observation of seismic waves of different polarization indicates subsurface anisotropy and might help to unravel its cause. *J. Applied Geophysics*, **30**, 1-24.

Li, Y. G., T. L. Teng, and T. L. Henyey, 1994: Shear-wave splitting observations in the northern Los Angles basin, southern California. *Bull. Seism. Soc. Am.*, **84**, 307-323.

Lynn, H. B., and L. A. Thomsen, 1990: Reflection shear-wave data collected near the principal axes of azimuthal anisotropy. *Geophysics*, **55**, 147-156.

MacBeth, C., X. Y. Li, X. Zeng, D. Cox, and J. Queen, 1997: Processing of a nine-component near-offset VSP for seismic anisotropy. *Geophysics*, **62**, 676-689.

Sayers, C. M., 1997: Determination of anisotropic velocity models from walkaway VSP data acquired in the presence of dip. *Geophysics*, **62**, 723-729.

Thomsen, L., 1986: Weak elastic anisotropy. *Geophysics*, **51**, 1954-1966.

Winterstein, D. F., and B. N. P. Paulsson, 1990: Velocity anisotropy in shale determined from crosshole seismic and vertical seismic profile data. *Geophysics*, **35**, 470-479.